2023 EAGE ANNUAL
84TH CONFERENCE & EXHIBITION
VIENNA | AUSTRIA

4D deghosting of multi-sensor streamer datasets from offshore Guyana

W. Zhao[1], P. Sadhnani[1], Y. Huang[1], S. Mothi[1], C.R. Schiott[2], S. Knapp[2], L. Vincent[2]

[1] CGG; [2] Hess Corporation

Summary

In 4D (time-lapse) imaging, the primary objective is to obtain a 4D image that is sufficiently free of noise associated with acquisition and processing in order to understand the changes at the reservoir interval. To obtain accurate 4D products, all seismic processing steps must effectively mitigate the differences arising from inconsistencies in acquisition setup and recording conditions of the time-lapse surveys. One of the key steps of the 4D processing sequence is deghosting, which is commonly used to remove the ghost variations between the baseline and monitor vintages. Deghosting can eliminate the variations in source and receiver tow depths and produce normalized broadband datasets at the same datum (mean sea level), which serve as input for further co-processing.

We present a 4D multi-sensor deghosting algorithm as an extension of recent deghosting technologies and apply it to a deep-tow multi-sensor streamer time-lapse survey acquired over the Liza field located offshore Guyana. The 4D image, which uses the proposed approach, shows significantly reduced 4D noise compared to result obtained with 3D deghosting of each vintage separately.

4D deghosting of multi-sensor streamer datasets from offshore Guyana

Introduction

In marine acquisition, source and receiver ghost wavefields interfere with the primary wavefield, resulting in undesirable notches over the seismic amplitude spectra, which limit access to the broadband information of the data. Deghosting, which removes the source and/or receiver ghost wavefields from the data, has become the norm in marine seismic imaging to recover the broadband signal for both single-component pressure data (Wang et al., 2014b) and multi-sensor pressure and velocity/ acceleration data (Poole, 2014; Wang et al., 2014a; Day et al., 2013). Deghosting is particularly important for time-lapse, or 4D, imaging (Loh et al., 2014) as different vintages are not recorded with the same source and receiver configurations or environmental conditions, e.g., sea-state variations. These differences can introduce significant non-repeatable 4D noise. We illustrate how we consolidate recent developments of deghosting technologies using the progressive sparse 3D Tau-P inversion scheme to achieve 4D deghosting of two multi-sensor vintage datasets. Using multi-sensor streamer data (Carlson et al., 2007) over the Liza field offshore Guyana, we demonstrate that 4D deghosting provides a better 4D image with much-improved signal-to-noise ratio (S/N) compared to 3D deghosting of each vintage separately.

Method

The progressive sparse 3D Tau-P inversion method (Wang et al., 2014b) effectively performs 3D deghosting of marine seismic data. This inversion scheme was extended to perform receiver- and source-side deghosting simultaneously, joint deghosting of multi-sensor hydrophone and accelerometer datasets (Wang et al., 2014a), and 4D deghosting of single-component pressure vintages (Wang et al., 2015), with the capability to handle receiver-side wave height variations (Poole and King, 2016). Building upon these deghosting technologies, we propose a scheme to perform 4D deghosting of multi-sensor vintages that also accounts for receiver-side wave height.

Multi-sensor streamer data can be classified into two main types: 1) pressure (P) and acceleration (A_Z and A_Y) and 2) pressure (P) and vertical velocity (V_Z). The joint deghosting scheme proposed in Equation 13 of Wang et al. (2014a) inverts for ghost-free data using the first type of multi-sensor streamer data (P, A_Z and A_Y) as the input, which can be modified to perform joint deghosting of pressure and vertical velocity data. The relationship between the pressure data P and vertical velocity data V_Z in $f-p$ domain is

$$P = \rho_w v_w V = \rho_w v_w \frac{V_z}{cos\theta} = \rho_w v_w \frac{V_z}{\sqrt{1-p_x^2 v_w^2 - p_y^2 v_w^2}}, \quad (1)$$

where ρ_w and v_w are the water density and velocity, respectively; p_x and p_y are the slownesses in x and y directions, respectively; and $cos\theta$ is the so-called obliquity operator that relates the vertical velocity V_Z to the total velocity V. A linear system for joint deghosting of P and V_Z can be written as

$$\begin{pmatrix} P \\ \rho_w v_w F_Z V_z \end{pmatrix} = \begin{pmatrix} LR_s R_{r,P} \\ F_Z L cos\theta R_s R_{r,Vz} \end{pmatrix} U, \quad (2)$$

where P and V_Z are input hydrophone and vertical velocity data, respectively, in $f-x$ domain with ghosts; U is ghost-free data in $f-p$ domain at the surface datum; R_s and R_r are the source- and receiver-side reghosting operators that add source and receiver ghosts to U, respectively; L is the inverse Tau-P operator; and F_Z is a band-pass filter to exclude low S/N frequency bands (mostly low frequencies) for vertical velocity V_Z data. Detailed explanations of the key operators L, R_s and R_r can be accessed in the previous works (Wang et al., 2014a, 2014b, 2015). The receiver-side wave-height variations (Poole and King, 2016) are included as part of the receiver-side reghosting operators, i.e., $r = r' + 2d_r$, where r' is the nominal receiver depth and d_r is the instantaneous wave-height estimated from P.

When there are two multi-sensor vintages (baseline data: P^b and V_z^b; monitor data: P^m and V_z^m), the scheme proposed in Equation 2 can be applied separately to baseline and monitor data to remove the ghosts in the two vintages for time-lapse processing (hereinafter, we call it 3D deghosting). We extend the 4D hydrophone-only deghosting algorithm proposed by Wang et al. (2015) to work with multi-sensor data as

$$\begin{pmatrix} P^b \\ \rho_w v_w F z V_z^b \\ P^m \\ \rho_w v_w F z V_z^m \end{pmatrix} = \begin{pmatrix} L^b R_s^b R_{r,P}^b & L^b R_s^b R_{r,P}^b & 0 \\ F_Z L^b cos\theta R_s^b R_{r,Vz}^b & F_Z L^b cos\theta R_s^b R_{r,Vz}^b & 0 \\ L^m R_s^m R_{r,P}^m & 0 & L^m R_s^m R_{r,P}^m \\ F_Z L^m cos\theta R_s^m R_{r,Vz}^m & 0 & F_Z L^m cos\theta R_s^m R_{r,Vz}^m \end{pmatrix} \begin{pmatrix} U^0 \\ U^b \\ U^m \end{pmatrix}, \quad (3)$$

where U^0 is the common ghost-free model, and U^b and U^m are remnant ghost-free models for the baseline and monitor, respectively. With this formulation, we can invert common events U^0 in both vintages simultaneously, in a consistent way, while preserving the 4D signals in U^b and U^m. Consistently deghosting the common events in different vintages is crucial in time-lapse processing. 3D deghosting of two vintages separately can lead to inconsistent deghosting of the common events and thus introduce 4D noise due to differences in acquisition configurations and environmental conditions. Data S/N also plays a role because deghosting is prone to instability at the ghost notches where S/N is low. Additionally, compared to 3D deghosting, 4D deghosting is better constrained with improved spatial sampling and notch diversity from multiple vintages.

Field Data Example

We tested our algorithm on multi-sensor (P and V_Z) time-lapse Liza field datasets located offshore Guyana. The Liza oil field is a deep-water discovery located in the Stabroek Block, approximately 190 km offshore Guyana, in water depths of 1500 m to 1900 m. The first discovery, Liza-1 well, was made in May 2015 (Alleyne et al., 2018). The Liza Phase 1 development project produced first oil in December 2019 with 17 producer/injector wells; and Phase 2 development started in February 2022. The 4D acquisitions used to perform time-lapse monitoring of Phase 1 production activities consisted of a baseline survey acquired in late 2017 (Knapp et al., 2022) and a monitor survey acquired in early 2022. Both datasets were designed to be acquired with the same narrow-azimuth multi-sensor configuration: tow depth of 20 m with a nominal cable spacing of 50 m, channel spacing of 12.5 m, and cable length of ~8 km. Both surveys used the same source configuration with a tow depth of 5 m. The monitor survey was set up to reproduce the acquisition configuration of the baseline survey as closely as possible to obtain good overall data repeatability.

3D deghosting and 4D deghosting were performed on the multi-sensor field datasets to produce ghost-free data. Kirchhoff migrations and image domain 4D QCs were performed on the baseline and monitor datasets obtained after each deghosting approach. The 4D difference of the reflectivity images were dominated by mid- to high-frequency components, while the relative impedance highlights the low-frequency component. In both types of 4D difference QCs, the 4D deghosting resulted in less 4D noise than the 3D deghosting. Clear improvement from 4D deghosting was observed for the low- and high-frequency components while for the mid-frequencies, where data S/N was relatively high, the uplift was more muted.

Overburden NRMS (normalized root mean square amplitude) QC was performed to quantify the quality uplift of 4D deghosting over 3D deghosting. As illustrated by Figure 1, the NRMS of the overburden reflectivity and relative impedance both show significant improvements in the 4D products with the proposed 4D deghosting. Based on the NRMS histograms, as illustrated by Figure 2, an approximately 2 percentage points reduction of NRMS was observed on the overburden reflectivity. On the low-frequency dominated relative impedance, we observed more than 3 percentage points reduction for NRMS.

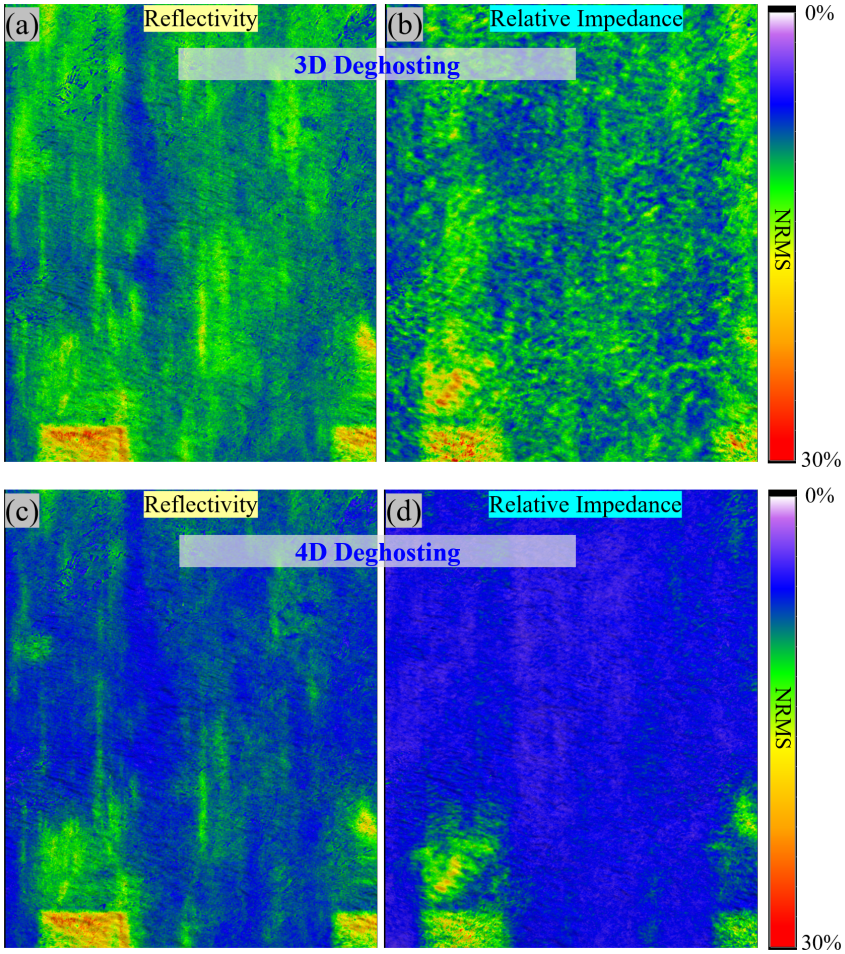

Figure 1 *Kirchhoff migration 4D NRMS plots based on 3D deghosting vs. 4D deghosting for overburden reflectivity ((a) and (c) respectively) and relative impedance ((b) and (d) respectively).*

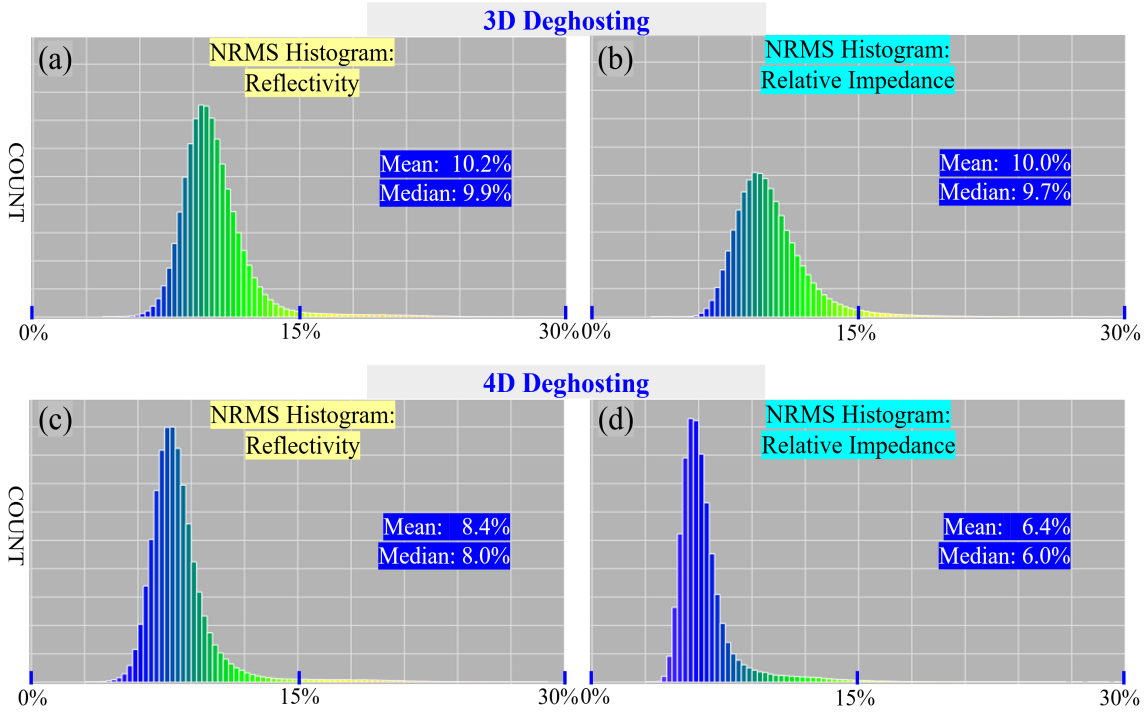

Figure 2 *Kirchhoff migration 4D NRMS histograms based on 3D deghosting vs. 4D deghosting for overburden reflectivity ((a) and (c) respectively) and relative impedance ((b) and (d) respectively).*

Note that 4D deghosting was an intermediate step in the 4D co-processing sequence. The NRMS is expected to be further enhanced with additional co-processing steps, such as multiple and residual noise attenuation. Furthermore, no post-processing was applied to the migration outputs as the focus was to evaluate the differences in the two deghosting approaches.

Conclusions and Discussions

Using a multi-sensor field data example, we have demonstrated that our consolidated 4D deghosting algorithm can significantly reduce the 4D noise compared to 3D deghosting. The maximum benefits of 4D deghosting were observed over the low- and high-frequency bands, where the data had an overall lower S/N. The success was due to (1) consistent deghosting of common events while preserving 4D signals and (2) better constrained inversion with increased spatial sampling and notch diversity from multiple vintages.

Further, several pre-processing steps, such as source designature (debubble and zero-phasing), channel amplitude correction, receiver motion correction, and water column correction, could be applied before deghosting. These steps can improve the timing and amplitude match between vintages, resulting in better 4D deghosted products.

Poor repeatability can limit the algorithm's capability to derive accurate "common events". Therefore, 4D deghosting has diminishing benefits in regions where the shot position repeatability is relatively poor, such as locations near the platform at the time of the shooting. Hence, acquiring repeatable surveys (mainly shot positions) still plays a vital role in 4D deghosting.

Acknowledgements

We thank Hess, ExxonMobil, CNOOC, and CGG for permission to publish this paper.

References

Alleyne, K., Layne, L. and Soroush, M. [2018]. Liza field development – The Guyanese perspective. *SPE Trinidad and Tobago Section Energy Resources Conference*, Expanded Abstracts, SPE-191239-MS.

Carlson, D., Long, A., Söllner, W., Tabti, H., Tenghamn, R. and Lunde, N. [2007]. Increased resolution and penetration from a towed dual-sensor streamer. *First Break*, 25(12), 71-77.

Day, A., Klüver, T., Söllner, W. and Carlson, D. [2013]. Wavefield-separation methods for dual-sensor towed-streamer data. *Geophysics*, 78(2), WA55-WA70.

Knapp, S., Vincent, L., Song, F. and Tang, Y. [2022]. Optimizing geophysical workflows; a case history of imaging success in the Guyana basin. *First EAGE Guyana-Suriname Basin Conference*, Extended Abstracts, D2-10.

Loh, F., Mojesky, T. and Bouloudas, P. [2014]. Full shot and receiver deghosting for Broadband and Conventional streamer 4D studies: How close can we get?. *84th SEG Annual International Meeting*, Expanded Abstracts, 4858-4862.

Poole, G. [2014]. Wavefield separation using hydrophone and particle velocity components with arbitrary orientation. *84th SEG Annual International Meeting*, Expanded Abstracts, 1858-1862.

Poole, G. and King, S. [2016]. Wave height guided multi-shot receiver deghosting. *87th SEG Annual International Meeting*, Expanded Abstracts, 4730-4734.

Wang, P., Jin, H, Peng, C. and Ray, S. [2014a]. Joint hydrophone and accelerometer receiver deghosting using sparse Tau-P inversion. *84th SEG Annual International Meeting*, Expanded Abstracts, 1894-1898.

Wang, P., Ray, S. and Nimsaila, K. [2014b]. 3D joint deghosting and crossline interpolation for marine single-component streamer data. *84th SEG Annual International Meeting*, Expanded Abstracts, 3594-3598.

Wang, P., Liu, J., Hembd, J. and Ray, S. [2015]. Joint 3D deghosting of multiple vintages. *85th SEG Annual International Meeting*, Expanded Abstracts, 5389-5393.